

Median Consensus Embedding for Dimensionality Reduction

Yui Tomo^{1*} and Daisuke Yoneoka¹

¹Center for Surveillance, Immunization, and Epidemiologic Research,
National Institute of Infectious Diseases, 1-23-1 Toyama, Shinjuku-Ku,
Tokyo 162-0052, Japan

*E-mail:tomoy@niid.go.jp

Abstract

This study proposes median consensus embedding (MCE) to address variability in low-dimensional embeddings caused by random initialization in dimensionality reduction techniques such as t -distributed stochastic neighbor embedding. MCE is defined as the geometric median of multiple embeddings. By assuming multiple embeddings as independent and identically distributed random samples and applying large deviation theory, we prove that MCE achieves consistency at an exponential rate. Furthermore, we develop a practical algorithm to implement MCE by constructing a distance function between embeddings based on the Frobenius norm of the pairwise distance matrix of data points. Application to real-world data demonstrates that MCE converges rapidly and significantly reduces instability. These results confirm that MCE effectively mitigates random initialization issues in embedding methods.

Keywords: Consensus embedding, Geometric median, High-dimensional data, Large deviations theory, Low-dimensional embedding, t -SNE, UMAP

1 Introduction

Dimensionality reduction methods, such as t -distributed stochastic neighbor embedding (t -SNE) and uniform manifold approximation and projection (UMAP), are widely used to visualize high-dimensional data (Van der Maaten and Hinton, 2008; McInnes et al., 2018). However, these nonlinear methods are sensitive to local optima, resulting in variability in embeddings even under the same parameter settings. This instability arises from random initialization, leading to instability in the results. Although strategies such as using the embedding of linear dimensionality reduction methods (e.g., principal component analysis) as initial values have been proposed to mitigate this issue, they remain ad hoc solutions (Kobak and Berens, 2019).

This study focuses on integrating multiple results obtained from various initializations to enhance stability. Similar integrative approaches are commonly employed in various statistical and machine learning fields. For example, in the development of prediction

models, ensemble-learning methods, such as bagging and boosting, are commonly used to achieve robust and stable results (Breiman, 1996; Freund and Schapire, 1995; Hastie et al., 2009). Similarly, in cluster analysis, consensus clustering or cluster ensemble approaches have been proposed to combine the outputs of clustering algorithms prone to initialization sensitivity, such as k -means, producing more robust and stable clustering results (Strehl and Ghosh, 2002).

In the context of integrating multiple low-dimensional embeddings, a consensus embedding approach has been proposed by Viswanath and Madabhushi (2012). Their method evaluates the "strength" of an embedding based on the extent to which the triangular relationships among data points in the high-dimensional space are preserved in the low-dimensional space. They also provide conditions for achieving a strong integrated embedding. However, their framework lacks a quantitative evaluation of the dependence of the results on random initializations. Moreover, it does not provide any statistical guarantee of the convergence rate toward a target embedding.

In this study, we propose median consensus embedding (MCE) as a novel approach for integrating multiple embeddings. MCE is defined as the geometric median of multiple embeddings. Specifically, the embedding that minimizes the average distance between them. By modeling each embedding as an independent and identically distributed (i.i.d.) sample from a probability measure and applying large-deviation theory, we prove that MCE converges consistently to the true embedding, defined as the expected embedding, at an exponential rate (Dembo and Zeitouni, 2009). This analysis extends previous work on the consensus clustering approach to the setting of consensus embedding (Topchy et al., 2004). We then construct a concrete distance function of embeddings based on the Frobenius norm of the pairwise distance matrix of the data points and develop a practical algorithm for implementing MCE. Finally, we evaluate the stability and convergence of our approach by applying it to real-world data.

2 Proposed Method

Let $\mathcal{Y} \subset \mathbb{R}^{n \times p}$ be a compact set, and let $y \in \mathcal{Y}$ represent an embedding. We assume that the embeddings remain invariant under rigid transformations and introduce the following equivalence relation \sim :

$$y_1 \sim y_2 \iff y_2^\top = R y_1^\top + \mathbf{1} v^\top \quad (R \in \Omega(p), v \in \mathcal{V}),$$

where $\Omega(p) \subset \mathbb{R}^{p \times p}$ denotes the set of all $p \times p$ orthogonal matrices, $\mathbf{1}$ is their p -dimensional column vector, and $\mathcal{V} \subset \mathbb{R}^n$ is a compact set. We introduce a set of equivalence classes denoted by $\tilde{\mathcal{Y}} = \mathcal{Y} / \sim$. Then, we define quotient mapping as:

$$\pi : \mathcal{Y} \rightarrow \tilde{\mathcal{Y}}, \quad \pi(y) = \{z \in \mathcal{Y} \mid z^\top = R y^\top + \mathbf{1} v^\top, R \in \Omega(p), v \in \mathcal{V}\}.$$

We hereafter consider embeddings as members of $\tilde{\mathcal{Y}}$. Subsequently, we define the function $d : \tilde{\mathcal{Y}} \times \tilde{\mathcal{Y}} \rightarrow \mathbb{R}_{\geq 0}$ that satisfies the following properties:

- (i) For all $y_1, y_2 \in \tilde{\mathcal{Y}}$, $d(y_1, y_2) = 0 \iff y_1 = y_2$. (Identifiability)
- (ii) For all $y_1, y_2 \in \tilde{\mathcal{Y}}$, $d(y_1, y_2) = d(y_2, y_1)$. (Symmetry)
- (iii) For all $y_1, y_2, y_3 \in \tilde{\mathcal{Y}}$, $d(y_1, y_2) + d(y_2, y_3) \geq d(y_1, y_3)$. (Triangle inequality)

Let μ be a probability measure on $\tilde{\mathcal{Y}}$, and suppose that the embeddings

$$y_1, y_2, \dots, y_m \in \tilde{\mathcal{Y}}$$

are i.i.d. random samples with μ . We define the true embedding y^* as the solution to the optimization problem:

$$y^* := \arg \min_{y \in \tilde{\mathcal{Y}}} \int_{\tilde{\mathcal{Y}}} d(y', y) d\mu(y').$$

Similarly, we define the median consensus embedding (MCE), represented by \hat{y} , as the minimizer

$$\hat{y} := \arg \min_{y \in \tilde{\mathcal{Y}}} \frac{1}{m} \sum_{i=1}^m d(y_i, y). \quad (1)$$

We then discuss the consistency of \hat{y} regarding true embedding y^* .

Remark 2.1. *Given that \mathcal{Y} , $\Omega(p)$, and \mathcal{V} are compact, the equivalence class $\pi(y)$ defined for each $y \in \mathcal{Y}$ is also compact. This follows because $\pi(y)$ is an image of a continuous mapping*

$$\Phi : \Omega(p) \times \mathcal{V} \rightarrow \mathcal{Y}, \quad \Phi(R, v) = (Ry^\top + \mathbf{1}v^\top)^\top.$$

Furthermore, because the mapping $\pi : \mathcal{Y} \rightarrow \tilde{\mathcal{Y}}$ is continuous and surjective, and \mathcal{Y} is compact, the quotient set $\tilde{\mathcal{Y}} = \mathcal{Y} / \sim$ is also compact.

3 Theoretical Analysis

3.1 Assumptions

First, we introduce the following assumptions:

Assumption 3.1 (Uniqueness of the true embedding). *For any $y \in \tilde{\mathcal{Y}} \setminus \{y^*\}$, we assume that:*

$$\int_{\tilde{\mathcal{Y}}} d(y', y) d\mu(y') > \int_{\tilde{\mathcal{Y}}} d(y', y^*) d\mu(y').$$

Assumption 3.2 (Existence of moment generating function). *Define $Z_y(y_i) := d(y_i, y^*) - d(y_i, y)$. Let $M_y(\lambda)$ denote the moment-generating function:*

$$M_y(\lambda) := \mathbb{E}_\mu [\exp(\lambda Z_y(y_i))].$$

We assume that for all $y \in \tilde{\mathcal{Y}}$ and $\lambda \in \mathbb{R}$, we obtain:

$$|M_y(\lambda)| < \infty.$$

3.2 Main Result

Under these assumptions, we establish the following theorem on MCE consistency:

Theorem 3.1 (Consistency with exponential rate). *Suppose that Assumptions 3.1 and 3.2 are satisfied, then for any $\epsilon > 0$, there exist $M \in \mathbb{N}$, $K > 0$, and $h > 0$ such that if $m > M$,*

$$\Pr(d(\hat{y}, y^*) \geq \epsilon) \leq K \exp(-mh).$$

Proof. For an i.i.d. random sequence $\{Z_y(y_i)\}_{i=1}^m$, where $Z_y(y_i) = d(y_i, y^*) - d(y_i, y)$, we define

$$\hat{S}_y^m := \frac{1}{m} \sum_{i=1}^m Z_y(y_i).$$

Based on Assumption 3.2, the logarithmic moment-generating function (cumulant-generating function) is given by:

$$\Lambda_y(\lambda) := \log M_y(\lambda) := \log \mathbb{E}_\mu[\exp(\lambda Z_y(y_i))] = \log \int_{\tilde{\mathcal{Y}}} \exp(\lambda Z_y(y'_i)) d\mu(y'_i).$$

The Fenchel-Legendre transform of $\Lambda_y(\lambda)$ is defined as:

$$\Lambda_y^*(z) := \sup_{\lambda \in \mathbb{R}} \{\lambda z - \Lambda_y(\lambda)\}.$$

The minimum value of $\Lambda_y^*(z)$ is 0 and only occurs at:

$$z = \bar{z}_y := \mathbb{E}_\mu[Z_y(y_i)] = \int_{\tilde{\mathcal{Y}}} \{d(y_i, y^*) - d(y_i, y)\} d\mu(y'_i) < 0, \quad \text{from Assumption 3.1.} \quad (2)$$

From Cramer's theorem (Theorem 2.2.3 and Corollary 2.2.19 in Dembo and Zeitouni (2009)), for any $y \in \tilde{\mathcal{Y}}$, we obtain:

$$\lim_{m \rightarrow \infty} \frac{1}{m} \log \Pr(\hat{S}_y^m \geq 0) = -\inf_{z \geq 0} \Lambda_y^*(z).$$

Thus, for any $\tau_y > 0$, there exists $M_y \in \mathbb{N}$ such that if $m \geq M_y$,

$$\Pr(\hat{S}_y^m \geq 0) \leq \exp\left(-m \left(\inf_{z \geq 0} \Lambda_y^*(z) - \tau_y\right)\right). \quad (3)$$

We define $\eta_y := \inf_{z \geq 0} \Lambda_y^*(z) - \tau_y$. Then, we have $\eta_y = \inf_{z \geq 0} \Lambda_y^*(z) - \tau_y > 0$ by choosing sufficiently small $\tau_y > 0$, because $\Lambda_y^*(z) > 0$ for $z \geq 0 > \bar{z}_y$ from (2).

From Lemma A.1, for any $\epsilon > 0$, there exist $N \in \mathbb{N}$ and points $y^{(1)}, \dots, y^{(N)} \in \{y \in \tilde{\mathcal{Y}} : d(y, y^*) \geq \epsilon\}$, and we obtain:

$$\Pr(d(\hat{y}, y^*) \geq \epsilon) \leq \sum_{j=1}^N \Pr(\hat{S}_{y^{(j)}}^m \geq 0).$$

By applying (3) to each $y^{(j)}$, we obtain:

$$\Pr(d(\hat{y}, y^*) \geq \epsilon) \leq \sum_{j=1}^N \exp(-m\eta_{y^{(j)}}) \leq N \exp(-m \min_{j=1, \dots, N} \eta_{y^{(j)}}), \quad \text{for } m > \max_{j=1, \dots, N} M_{y^{(j)}}.$$

Therefore, by defining $M = \max_{j=1, \dots, N} M_{y^{(j)}} \in \mathbb{N}$, $K = N > 0$, and $h = \min_{j=1, \dots, N} \eta_{y^{(j)}} > 0$, we conclude that if $m > M$,

$$\Pr(d(\hat{y}, y^*) \geq \epsilon) \leq K \exp(-mh).$$

□

4 Algorithm Construction

We develop a practical algorithm for applying MCE to real-world data.

4.1 Reformulation of the Optimization Problem

We define the mapping $X : \mathcal{Y} \rightarrow \mathcal{X} \subset \mathbb{R}^{n \times n}$ as:

$$X(y)_{(ij)} := \|y_{(i)} - y_{(j)}\|, \quad \text{for } i, j = 1, \dots, n, \quad (4)$$

where $X(y)_{(ij)}$ denotes the (i, j) th entry of $X(y)$ and $y_{(i)}$ is the i th row of $y \in \mathcal{Y}$. Furthermore, we define the mapping $\tilde{X} : \tilde{\mathcal{Y}} \rightarrow \mathcal{X}$ as

$$\tilde{X}(y) := X(y'),$$

where $y' \in \mathcal{Y}$ is a representative of $y \in \tilde{\mathcal{Y}}$.

Remark 4.1. *Given that \mathcal{Y} is compact and X is continuous; thus, \mathcal{X} is also compact.*

Let $D : \mathcal{X} \times \mathcal{X} \rightarrow \mathbb{R}_{\geq 0}$ be a continuous function satisfying identifiability, symmetry, and triangle inequalities. We then define the distance functions $d : \tilde{\mathcal{Y}} \times \tilde{\mathcal{Y}} \rightarrow \mathbb{R}_{\geq 0}$ as:

$$d(y_1, y_2) := D\left(\tilde{X}(y_1), \tilde{X}(y_2)\right).$$

We define the optimization problem based on D as:

$$\hat{x} := \arg \min_{x \in \mathcal{X}} \frac{1}{m} \sum_{i=1}^m D(x_i, x), \quad (5)$$

where $x_i := \tilde{X}(y_i)$ for $y_1, \dots, y_m \in \tilde{\mathcal{Y}}$. We now establish the following proposition regarding the equivalence of the optimization problems:

Proposition 4.1 (Equivalence of optimization problems). *Let \hat{y} be the solution to the optimization problem (1) and \hat{x} be the solution to (5). Then, it holds that $\tilde{X}(\hat{y}) = \hat{x}$.*

Proof. As the embeddings are invariant under rigid transformations, if $z \in \pi(y)$ for $y \in \mathcal{Y}$, then $X(z) = X(y)$. Consequently, the mapping $\tilde{X} : \tilde{\mathcal{Y}} \rightarrow \mathcal{X}$ is bijective. For any $x = \tilde{X}(y)$ with $y \in \tilde{\mathcal{Y}}$ and $x_i = \tilde{X}(y_i)$ for $y_1, \dots, y_m \in \tilde{\mathcal{Y}}$, the objective function can be rewritten as:

$$\frac{1}{m} \sum_{i=1}^m d(y_i, y) = \frac{1}{m} \sum_{i=1}^m D\left(\tilde{X}(y_i), \tilde{X}(y)\right) = \frac{1}{m} \sum_{i=1}^m D(x_i, x).$$

Therefore, the optimization problems (1) and (5) are equivalent, implying that $\tilde{X}(\hat{y}) = \hat{x}$. \square

4.2 Implementation Algorithm

The reformulated optimization problem (5) using Proposition 4.1 corresponds to the computation of the geometric median in the feature space \mathcal{X} . This can be numerically solved using the Weiszfeld algorithm.

As a concrete distance function $D : \mathcal{X} \times \mathcal{X} \rightarrow \mathbb{R}_{\geq 0}$, we use the Frobenius norm

$$D(x_1, x_2) = \|x_1 - x_2\|_F, \quad \text{for } x_1, x_2 \in \mathcal{X} \subset \mathbb{R}^{n \times n}.$$

The solution \hat{x} can be visualized in \mathbb{R}^2 via multi-dimensional scaling (MDS). Based on these components, we construct a practical MCE algorithm as Algorithm 1.

The computational cost of the initial computation of the distance matrices for each embedding is $\mathcal{O}(m n^2)$. In each iteration of the Weiszfeld algorithm, computing the Frobenius norm for each distance matrix requires $\mathcal{O}(m n^2)$ operations. Therefore, if T iterations are required, the computational cost of this step is $\mathcal{O}(T m n^2)$. Finally, the MDS step involves the eigen decomposition of an $n \times n$ matrix, which typically has a cost of $\mathcal{O}(n^3)$. Therefore, the total computational cost is $\mathcal{O}((T + 1) m n^2 + n^3)$.

5 Application to Actual Data

We apply the MCE method, as implemented in Algorithm 1, to actual data. We demonstrate a rapid convergence and reduction in embedding instability for increase in the number of integrated embeddings.

5.1 Data

We utilize the Digit Dataset, an 8×8 pixel handwritten digit dataset available in the Python library scikit-learn (Pedregosa et al., 2011). The dataset consists of 1,797 samples spanning digit classes 0–9, with each sample represented as a 64-dimensional vector of pixel values.

5.2 Methods

We first applied t-SNE to embed the digit data in two dimensions 1000 times with different random initializations. We then performed MCE using these 1000 embeddings as inputs, denoting the results as \hat{y}_{1000} . We then obtained 5 different embeddings using t-SNE and MCE with 2, 10, 20, 50, 100 embeddings from the t-SNE. If $\{\hat{y}_{(1)}, \dots, \hat{y}_{(5)}\}$ denotes a set of 5 different embeddings, we calculated the following quantity:

- (1) Mean distance to \hat{y}_{1000} : $\sum_{i=1}^5 d(\hat{y}_{(i)}, \hat{y}_{1000})$.
- (2) Mean pairwise distance among embeddings: $\sum_{1 \leq i < j \leq 5} d(\hat{y}_{(i)}, \hat{y}_{(j)})$.

t-SNE was performed using scikit-learn with the perplexity parameter set to 30. The initial values were generated as the default setting of the library, from a 2-dimensional normal distribution $\mathcal{MVN}(\mathbf{0}, 10^{-4} \times I)$, where $\mathbf{0}$ denotes the zero vector and I is the 2-dimensional identity matrix. The MCE was implemented in Python 3.8.3 using Algorithm 1.

5.3 Results

Figure 1 shows a visualization of \hat{y}_{1000} . Figure 2 shows the visualizations of different 5 embeddings obtained using t-SNE and MCE with 2, 10, 20, 50, 100 embeddings from t-SNE. Each embedding was aligned with \hat{y}_{1000} using Procrustes analysis. In these figures, the color of each point corresponds to the digit class label (0–9).

The mean distances to \hat{y}_{1000} were 21591.02 (t-SNE), 13012.06 (MCE with 2 t-SNE embeddings), 6920.66 (MCE with 10 t-SNE embeddings), 5832.52 (MCE with 20 t-SNE embeddings), 4593.57 (MCE with 50 t-SNE embeddings), and 2892.45 (MCE with 100 t-SNE embeddings). The mean pairwise distances were 29823.75 (t-SNE), 19657.76 (MCE with 2 t-SNE embeddings), 9585.07 (MCE with 10 t-SNE), 7390.42 (MCE with 20 t-SNE embeddings), 5953.69 (MCE with 50 t-SNE embeddings), and 3790.76 (MCE with 100 t-SNE embeddings). These values are plotted in Figure 3.

These results indicate a rapid convergence and reduction in embedding instability for the MCE with the number of integrated embeddings. Both evaluation metrics decreased sharply up to $m = 10$, after which the rate of decrease gradually declined. Consequently, using approximately $m = 10$ may be sufficient for achieving adequate integration quality.

6 Discussion

In this study, we propose an MCE method for integrating multiple embeddings. By modeling them as i.i.d. samples from a probability measure and applying large deviation theory, our approach achieves consistency at an exponential rate. Furthermore, we construct a practical algorithm based on the Frobenius norm of the pairwise distance matrix of the data points. Applying this method to real data, we demonstrate that as the number of embeddings m increases, embedding variability decreases. These results indicate that the consensus-embedding framework using a geometric median can effectively mitigate the instability of embeddings caused by random initialization and enhance the reliability of high-dimensional data analysis.

The MCE is applicable to other settings. For example, t-SNE is highly sensitive to the perplexity parameter, which can be addressed by integrating the embeddings obtained using multiple perplexity settings. Although multiscale t-SNE has been proposed to address this issue by averaging the similarity probability models of data points in high-dimensional space, it does not address issues related to parameter settings in the optimization process (Lee et al., 2015). Our approach addresses both of these issues. Similarly, UMAP is influenced by tuning parameters, and integrating the embeddings obtained with different parameter settings can address similar problems. However, if the tuning parameter settings are deterministic, the theoretical guarantees established in this study cannot be applied. Furthermore, it may be possible to mitigate missing values in the embedding by integrating the embeddings obtained from multiple imputed datasets, as well as approaches that combine multiple imputation and consensus clustering methods for clustering with missing data (Audigier and Niang, 2023).

To apply these theoretical results, we must consider the following assumptions: In Assumption 3.1, we define the distance space on $\tilde{\mathcal{Y}}$ rather than \mathcal{Y} to ensure invariance under rigid transformations. Therefore, if we assume the continuity of $\mu(y)$, it follows that almost surely,

$$\int_{\tilde{\mathcal{Y}}} d(y', y) d\mu(y') \neq \int_{\tilde{\mathcal{Y}}} d(y', y^*) d\mu(y'),$$

when $y \neq y^*$. Assumption 3.2 may not hold if the underlying distribution of $Z_y(y_i)$ has a heavy tail.

The definition of true embedding used in this study differs from that in Viswanath and Madabhushi (2012). In this study, we define true as the minimization of the expected distance regarding a probability measure. Although this formulation is natural from a

statistical perspective, it does not guarantee improvements in embedding evaluation metrics. Some metrics for low-dimensional embeddings evaluate local neighborhood structure preservation, such as the average K-ary neighborhood preservation and co-k-nearest neighbor size, whereas others access cluster structure using label information, such as the silhouette coefficient (Lee and Verleysen, 2009; Zhang et al., 2021; Rousseeuw, 1987). Future work will explore the practical properties of MCE across various datasets and evaluation metrics.

Although MCE can reduce the variability caused by random initialization, the results still depend on the probabilistic model used to generate the initial values. Nonlinear dimensionality reduction methods typically generate low-dimensional embeddings that preserve certain structural properties of high-dimensional space. For example, t-SNE and UMAP prioritize local neighborhood structure preservation of each data point. Consequently, global structures are typically lost in the resulting embeddings. However, studies suggest that selecting appropriate initial values can enhance global structure preservation (Kobak and Berens, 2019). Investigating better initialization models remains a topic for future research.

Acknowledgement

We would like to thank Editage (www.editage.jp) for English language editing.

Disclosure statement

The authors declare no conflicts of interest.

Code Availability

The Python implementation of MCE is available at <https://github.com/t-yui/MedianConsensusEmbedding>.

A Technical Lemma

We establish the following lemma for Theorem 3.1.

Lemma A.1. *For any $\varepsilon > 0$, there exist $N \in \mathbb{N}$ and the points $y^{(1)}, \dots, y^{(N)} \in \{y \in \tilde{\mathcal{Y}} : d(y, y^*) \geq \varepsilon\}$ such that*

$$\Pr(d(\hat{y}, y^*) \geq \varepsilon) \leq \sum_{j=1}^N \Pr(\hat{S}_{y^{(j)}}^m \geq 0).$$

Proof. As $\tilde{\mathcal{Y}}$ is compact, $A := \{y \in \tilde{\mathcal{Y}} : d(y, y^*) \geq \varepsilon\}$ is also compact. According to the Heine–Cantor theorem, the function

$$f(y) := \frac{1}{m} \sum_{i=1}^m d(y_i, y)$$

is uniformly continuous in $\tilde{\mathcal{Y}}$.

We assume $d(\hat{y}, y^*) \geq \varepsilon$. Then, by the uniform continuity of f , for any $\eta > 0$, there exists $\delta > 0$ such that for all $y, y' \in \tilde{\mathcal{Y}}$,

$$d(y, y') < \delta \implies |f(y) - f(y')| < \eta.$$

Furthermore, based on the definition of compactness, a finite collection of open balls exists:

$$B(y^{(j)}, \delta) = \{z \in \tilde{\mathcal{Y}} : d(z, y^{(j)}) < \delta\}, \quad y^{(j)} \in A, \quad j = 1, \dots, N_\delta \in \mathbb{N},$$

such that

$$A \subset \bigcup_{j=1}^{N_\delta} B(y^{(j)}, \delta).$$

Because $\hat{y} \in A$, there exists some $j \in \{1, \dots, N_\delta\}$ for which

$$d(\hat{y}, y^{(j)}) < \delta.$$

Then, by using the uniform continuity of f , we have

$$|f(\hat{y}) - f(y^{(j)})| < \eta.$$

Because \hat{y} is a minimizer of f , it follows that:

$$f(\hat{y}) \leq f(y^{(j)}),$$

and hence,

$$f(y^{(j)}) < f(\hat{y}) + \eta.$$

Furthermore, as $f(\hat{y}) \leq f(y^*)$, we obtain

$$f(y^{(j)}) < f(y^*) + \eta,$$

namely,

$$\hat{S}_{y^{(j)}}^m = f(y^*) - f(y^{(j)}) > -\eta.$$

Suppose that $\hat{S}_{y^{(j)}}^m < 0$. Then there exists $\gamma > 0$ such that

$$\hat{S}_{y^{(j)}}^m \leq -\gamma.$$

As we can choose $\eta > 0$ arbitrarily, we choose $\eta = \gamma/2$, which results in

$$-\gamma \geq \hat{S}_{y^{(j)}}^m > -\frac{\gamma}{2},$$

which is contradictory. Therefore, $\hat{S}_{y^{(j)}}^m \geq 0$.

From the discussion above, if $d(\hat{y}, y^*) \geq \varepsilon$, then there exists $N \in \mathbb{N}$ and $y^{(j)} \in A$ such that $\hat{S}_{y^{(j)}}^m \geq 0$; that is,

$$\{d(\hat{y}, y^*) \geq \varepsilon\} \subset \bigcup_{j=1}^N \{\hat{S}_{y^{(j)}}^m \geq 0\}.$$

Taking the probabilities on both sides, we obtain

$$\Pr(d(\hat{y}, y^*) \geq \varepsilon) \leq \sum_{j=1}^N \Pr(\hat{S}_{y^{(j)}}^m \geq 0).$$

□

References

- Audigier, V. and Niang, N. (2023). Clustering with missing data: Which equivalent for rubin’s rules? *Advances in Data Analysis and Classification*, 17:623–657.
- Breiman, L. (1996). Bagging predictors. *Machine learning*, 24:123–140.
- Dembo, A. and Zeitouni, O. (2009). *Large deviations techniques and applications*, volume 38. Springer Science & Business Media.
- Freund, Y. and Schapire, R. E. (1995). A decision-theoretic generalization of on-line learning and an application to boosting. In *European conference on computational learning theory*, pages 23–37. Springer.
- Hastie, T., Tibshirani, R., Friedman, J., Hastie, T., Tibshirani, R., and Friedman, J. (2009). Ensemble learning. *The elements of statistical learning: data mining, inference, and prediction*, pages 605–624.
- Kobak, D. and Berens, P. (2019). The art of using t-sne for single-cell transcriptomics. *Nature communications*, 10(1):5416.
- Lee, J. A., Peluffo-Ordóñez, D. H., and Verleysen, M. (2015). Multi-scale similarities in stochastic neighbour embedding: Reducing dimensionality while preserving both local and global structure. *Neurocomputing*, 169(2):246–261.
- Lee, J. A. and Verleysen, M. (2009). Quality assessment of dimensionality reduction: Rank-based criteria. *Neurocomputing*, 72(7-9):1431–1443.
- McInnes, L., Healy, J., and Melville, J. (2018). Umap: Uniform manifold approximation and projection for dimension reduction. *arXiv preprint arXiv:1802.03426*.
- Pedregosa, F., Varoquaux, G., Gramfort, A., Michel, V., Thirion, B., Grisel, O., Blondel, M., Prettenhofer, P., Weiss, R., Dubourg, V., Vanderplas, J., Passos, A., Cournapeau, D., Brucher, M., Perrot, M., and Duchesnay, E. (2011). Scikit-learn: Machine learning in Python. *Journal of Machine Learning Research*, 12:2825–2830.
- Rousseeuw, P. J. (1987). Silhouettes: a graphical aid to the interpretation and validation of cluster analysis. *Journal of computational and applied mathematics*, 20:53–65.
- Strehl, A. and Ghosh, J. (2002). Cluster ensembles—a knowledge reuse framework for combining multiple partitions. *Journal of machine learning research*, 3(Dec):583–617.
- Topchy, A. P., Law, M. H., Jain, A. K., and Fred, A. L. (2004). Analysis of consensus partition in cluster ensemble. In *Fourth IEEE International Conference on Data Mining (ICDM’04)*, pages 225–232. IEEE.
- Van der Maaten, L. and Hinton, G. (2008). Visualizing data using t-sne. *Journal of machine learning research*, 9(11):2579–2605.
- Viswanath, S. and Madabhushi, A. (2012). Consensus embedding: theory, algorithms and application to segmentation and classification of biomedical data. *BMC bioinformatics*, 13:1–20.
- Zhang, Y., Shang, Q., and Zhang, G. (2021). pyDRMetrics—a python toolkit for dimensionality reduction quality assessment. *Heliyon*, 7(2).

Algorithm 1 Implementation of MCE

Require: Embeddings y_1, y_2, \dots, y_m and a sufficiently small constant $\varepsilon > 0$

Ensure: Optimal distance matrix \hat{x} and the corresponding embedding \hat{y}

```
1: for  $i = 1$  to  $m$  do
2:   for  $k = 1$  to  $n$  do
3:     for  $l = 1$  to  $n$  do
4:        $X(y_i)_{(k,l)} \leftarrow \|y_{i(k)} - y_{i(l)}\|$ 
5:     end for
6:   end for
7: end for
8:  $x^{(0)} \leftarrow \frac{1}{m} \sum_{i=1}^m X(y_i)$ 
9: for  $t = 1$  to maximum number of iterations do
10:   $w_i \leftarrow 1 / (\|x^{(t-1)} - X(y_i)\|_F + \varepsilon)$ 
11:   $x^{(t)} \leftarrow \sum_{i=1}^m w_i X(y_i) / \sum_{i=1}^m w_i$ 
12:  if the convergence criterion is satisfied then
13:    break
14:  end if
15: end for
16:  $\hat{x} \leftarrow x^{(t)}$ 
17:  $\hat{y} \leftarrow \text{MultiDimensionalScaling}(\hat{x})$ 
18: return  $\hat{x}, \hat{y}$ 
```

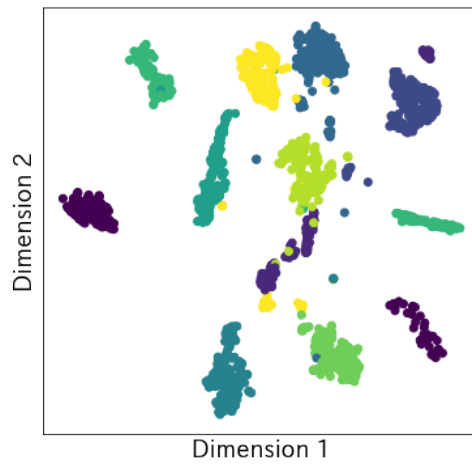
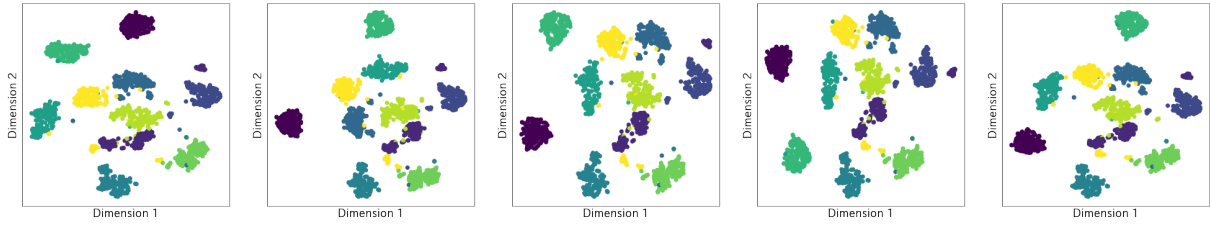
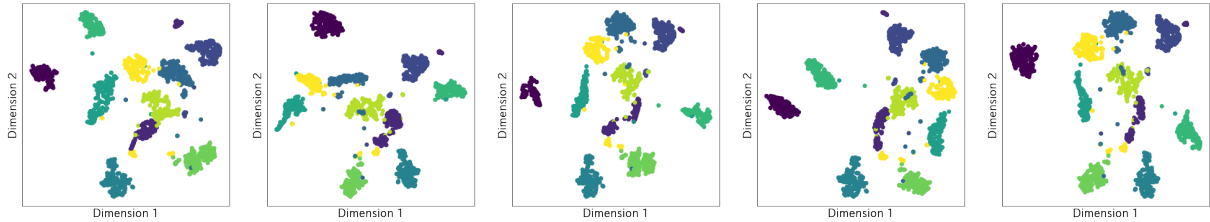


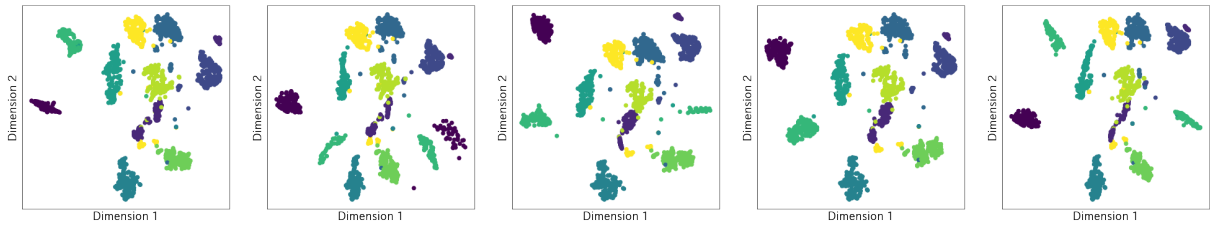
Figure 1: Visualization of the embedding of the Digits data obtained by the MCE with 1000 t-SNE embeddings. Each point is colored according to its corresponding handwritten digit class (0-9).



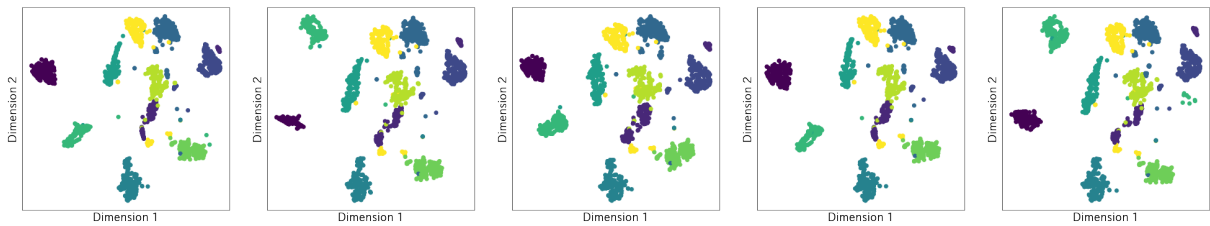
(a) 5 t-SNE embeddings with random initialization



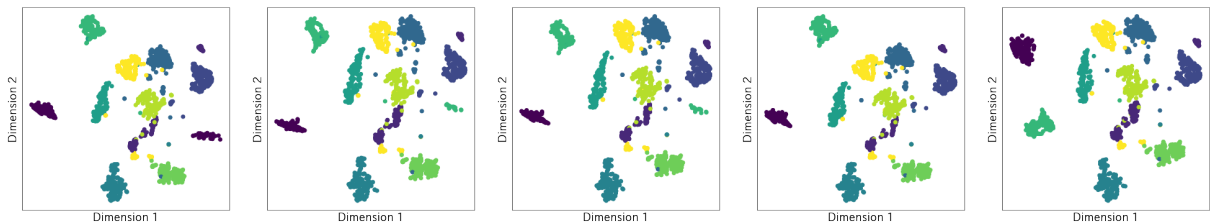
(b) 5 MCE embeddings with 2 embeddings of t-SNE



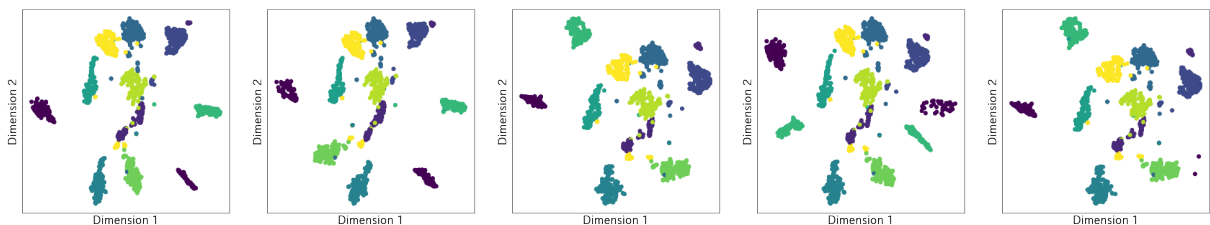
(c) 5 MCE embeddings with 10 embeddings of t-SNE



(d) 5 MCE embeddings with 20 embeddings of t-SNE

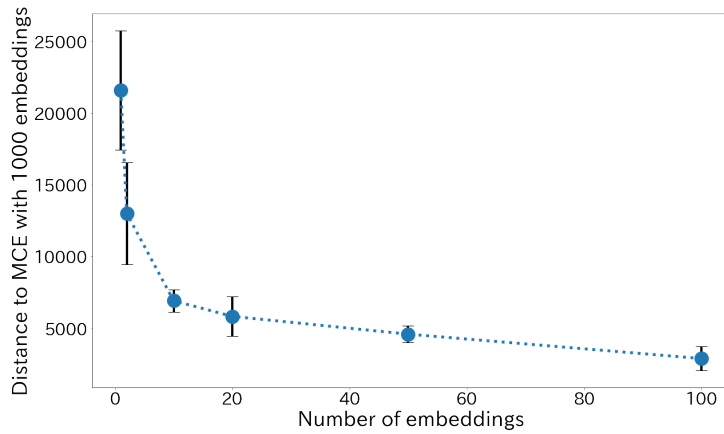


(e) 5 MCE embeddings with 50 embeddings of t-SNE

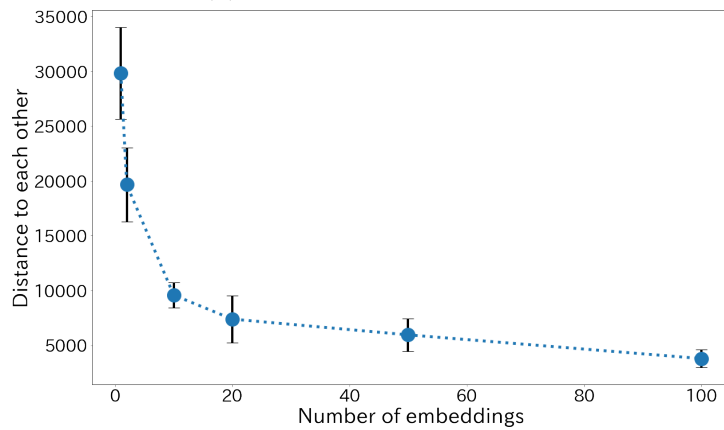


(f) 5 MCE embeddings with 100 embeddings of t-SNE

Figure 2: Embeddings of the Digits data obtained by t-SNE and MCE with different initializations. The embeddings of MCE were obtained by integrating multiple t-SNE embeddings of the Digits data ($m = 2, 10, 20, 50, 100$).



(a) Mean distance to \hat{y}_{1000}



(b) Mean pairwise distance among embeddings

Figure 3: Mean distance to \hat{y}_{1000} and mean pairwise distance among embeddings for t-SNE embeddings and MCE embeddings ($m = 2, 10, 20, 50, 100$). The results are shown with error bars indicating standard deviations (SD).